Chemical Engineering Journal 333 (2018) 146–152

Contents lists available at ScienceDirect

Chemical Engineering Journal

journal homepage: www.elsevier.com/locate/cej

Flow fabrication of a highly efficient Pd/UiO-66-NH_2 film capillary microreactor for 4-nitrophenol reduction

Jing Li[a], Feichao Wu[a], Lu Lin[a], Yu Guo[b,*], Haiou Liu[a], Xiongfu Zhang[a,*]

[a] State Key Laboratory of Fine Chemicals, School of Chemical Engineering, Dalian University of Technology, Dalian 116024, China
[b] School of Chemical and Environmental Engineering, Liaoning University of Technology, Jinzhou 121001, China

GRAPHICAL ABSTRACT

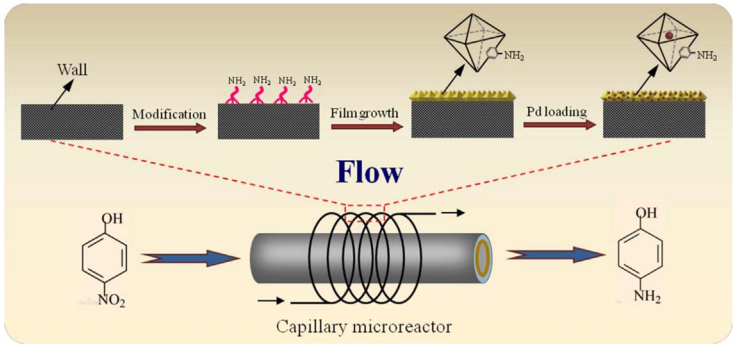

ARTICLE INFO

Keywords:
Microreactor
Pd nanoparticles
UiO-66-NH_2 film
Flow synthesis
Catalytic hydrogenation

ABSTRACT

A novel Pd/UiO-66-NH_2 film quartz capillary microreactor was fabricated by a flow method in which fine control of the film thickness and metal loading could be readily achieved by adjusting flow time. Firstly, UiO-66-NH_2 film as the catalyst support layer was synthesized on the inner wall of the quartz capillary employing a two-step procedure including surface modification with 3-aminopropyltriethoxysilane (APTES) and the subsequent flow growth of UiO-66-NH_2 film. Secondly, Pd nanoparticles (NPs) were uniformly and firmly immobilized in the UiO-66-NH_2 film as active catalysts using the same flow method. Such Pd/UiO-66-NH_2 film capillary microreactor was applied as catalyst for the reduction of 4-nitrophenol (4-NP) to produce 4-aminophenol (4-AP) under continuous flow conditions. Nearly 100% conversion was achieved under mild conditions in a short residence time. Importantly, no deactivation was observed for this microreactor during the continuous flow reaction of 100 h, indicating its excellent stability due to the firm immobilization of active Pd NPs in UiO-66-NH_2 film.

1. Introduction

Membrane/film microreactors, fabricated by assembling membranes/films in catalytic configurations with channels below 500 μm in diameter, have attracted increasing interest as highly efficient heterogeneous catalysts [1–5]. First of all, microreactor itself can offer enhanced catalytic performance due to its intrinsically higher mass and heat transfer rate [6]. Then, the introduction of membrane/film in microreactors can realize the immobilization and uniform dispersion of catalytic active components, and achieve supra-equilibrium conversions, resulting in intensified production processes and greatly improved reaction efficiency [7,8]. Furthermore, the coated membrane/film, as a protective layer, can also prevent metal nanocatalysts from deactivation by avoiding aggregation and leaching of active

* Corresponding authors.
E-mail addresses: guoyulnut@163.com (Y. Guo), xfzhang@dlut.edu.cn (X. Zhang).

http://dx.doi.org/10.1016/j.cej.2017.09.154
Received 16 August 2017; Received in revised form 22 September 2017; Accepted 24 September 2017
Available online 25 September 2017
1385-8947/

nanoparticles [9,10]. Such membrane/film-based microreactors can generally be synthesized either by static method or under flow condition. The latter approach is preferred over the former one because of its merits in achieving continuous and uniform membrane/film layers on the inner surface of the microreactors with huge ratio of length to diameter.

Metal organic frameworks (MOFs), constructed by the periodic coordination of metal ions/clusters and ligands, possess uniform microporous structure, large surface areas and even some acidic or basic sites [11,12]. These advantages have inspired researchers to explore their potential as membrane/film substrates for loading catalytically active components. For example, Mao et al. [9] firstly employed HKUST-1, a MOF material, in the form of film to immobilize various functional particles (metal nanoparticles, inorganic, polymers, proteins and so on) for catalysis and bio-activity application. Zamaro and co-workers [10] achieved ZIF-8 films on microchannel copper foils to support Ag nanoparticles and then conducted the composite films as high-performance catalysts in the CO oxidation. Despite the efforts have been devoted, much work still needs to be done on more types of appropriate MOFs to explore their potential as membrane/film supports in microreactors. The UiO-66 family, composed of $Zr_6O_4(OH)_4$ cluster and carboxylate ligands, exhibits exceptional chemical and thermal stabilities [13,14]. Besides, UiO-66 and its derivative materials are also widely used as supports to encapsulate active catalytic species [15–18]. Therefore, these Zr-based crystalline materials may serve as a promising candidate for membrane/film substrates. However, to the best of our knowledge, there are few reports about the coating of UiO-66 series MOFs on microchannels as membrane/film microreactors for catalytic application.

In the present work, a facile flow method was developed to fabricate a highly efficient capillary quartz microreactor based on Pd nanoparticles (NPs) immobilized in UiO-66-NH_2 film (named as Pd/UiO-66-NH_2 film) for 4-nitrophenol reduction. As shown in Fig. 1, the method involves a two-step procedure including the growth of a continuous UiO-66-NH_2 film on the inner surface of quartz capillary, followed by immobilizing active Pd species inside the UiO-66-NH_2 film. The thickness of the UiO-66-NH_2 film and the loading content of Pd NPs could be conveniently optimized by adjusting the operation time to achieve highly efficient capillary microreactor. This method covered three key points: 1) APTES was employed to chemically modify the inner surface of the quartz capillary with active nucleation and growth sites for the formation of a continuous and uniform UiO-66-NH_2 film; 2) porous UiO-66-NH_2 film was selected as the support for fixing Pd species because UiO-66-NH_2 has functional amino groups to immobilize Pd NPs without agglomeration and leaching through metal coordination chelation [17,19]; 3) all procedures including the preparation of the Pd/UiO-66-NH_2 film catalyst and reaction of 4-nitrophenol reduction were conducted under flow conditions, which was simple and scalable. The reduction of 4-nitrophenol with $NaBH_4$, a part of the catalytic hydrogenation of aromatic nitro compounds, is usually served as the standard of testing nanostructured catalysts and exploiting for the study of catalytic activities [20–21]. This reaction can not only be carried out under ambient conditions without by-products, but also can be facile analyzed by UV–Vis spectroscopy [22]. Moreover, *p*-aminophenol is also an important intermediate [23].

2. Experimental

2.1. Materials

The quartz capillaries (O. D: 630 μm, I. D: 530 μm, length: 250 mm) were purchased from Dalian Zhong Hui Da Instrument Corporation. 3-aminopropyltriethoxysilane (APTES), Zirconium tetrachloride ($ZrCl_4$), *N,N*-Dimethylformamide (DMF), 2-aminoterephthalic acid (NH_2-H_2BDC), acetic acid (99.5%) were obtained from Sigma Aldrich. 4-nitrophenol (4-NP), sodium borohydride ($NaBH_4$), hydrochloric acid (HCl), sodium hydroxide (NaOH) and ethyl alcohol were supplied by Sinopharm Chemical Reagents Co. Ltd. (Beijing, China). Palladium chloride ($PdCl_2$) was obtained from Shanghai Jiuling Chemical Co. Ltd. (Shanghai, China). All the chemical reagents were used as received without further purification. The used deionized water (DI water) was home-made.

2.2. Fabrication of Pd/UiO-66-NH_2 film microreactors by the flow method

2.2.1. Synthesis of UiO-66-NH_2 film on the inner wall

The quartz capillary was used as a microchannel for the flow growth of UiO-66-NH_2 film including chemical surface modification of the internal surface of the quartz capillary and then the growth of UiO-66-NH_2film. As shown in Fig. 2, a homemade device was employed for the film growth. At first, the quartz capillary was successively pre-treated with 1.0 M HCl and 1.0 M NaOH at 348 K, and then APTES was grafted on the surface of the wall by pumping the mixture solution of APTES and ethyl alcohol (1:30 v/v) at a velocity of 1 mL/h for 3 h at 348 K.

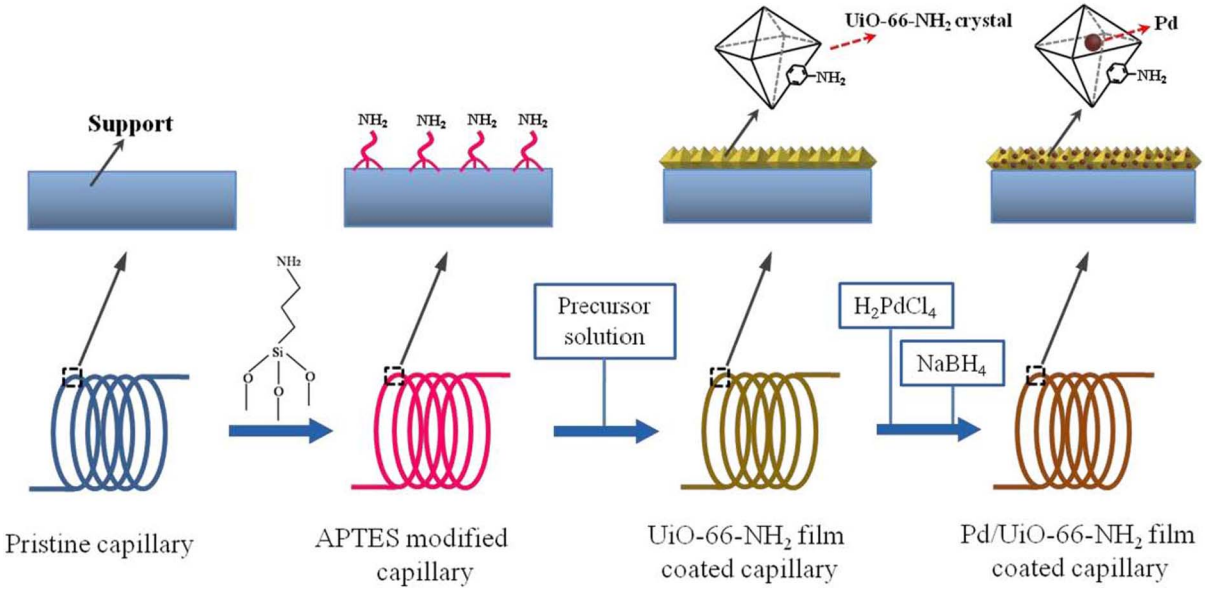

Fig. 1. Schematic representation of the fabrication process.

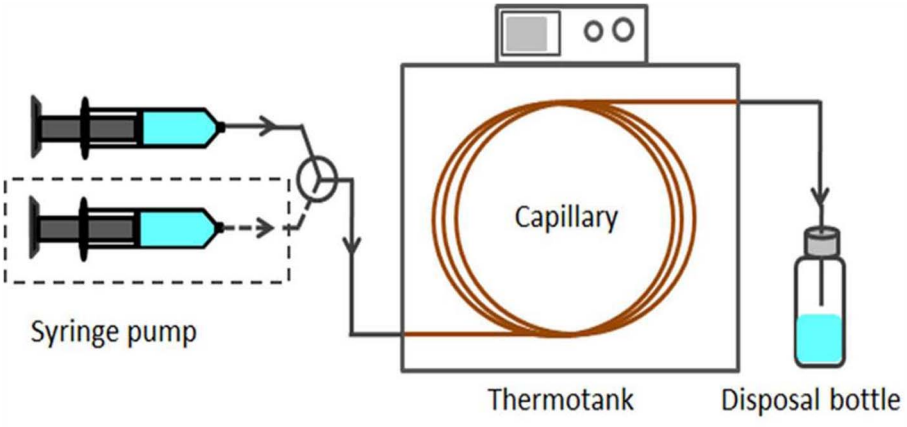

Fig. 2. Flow synthesis device for capillary microreactor.

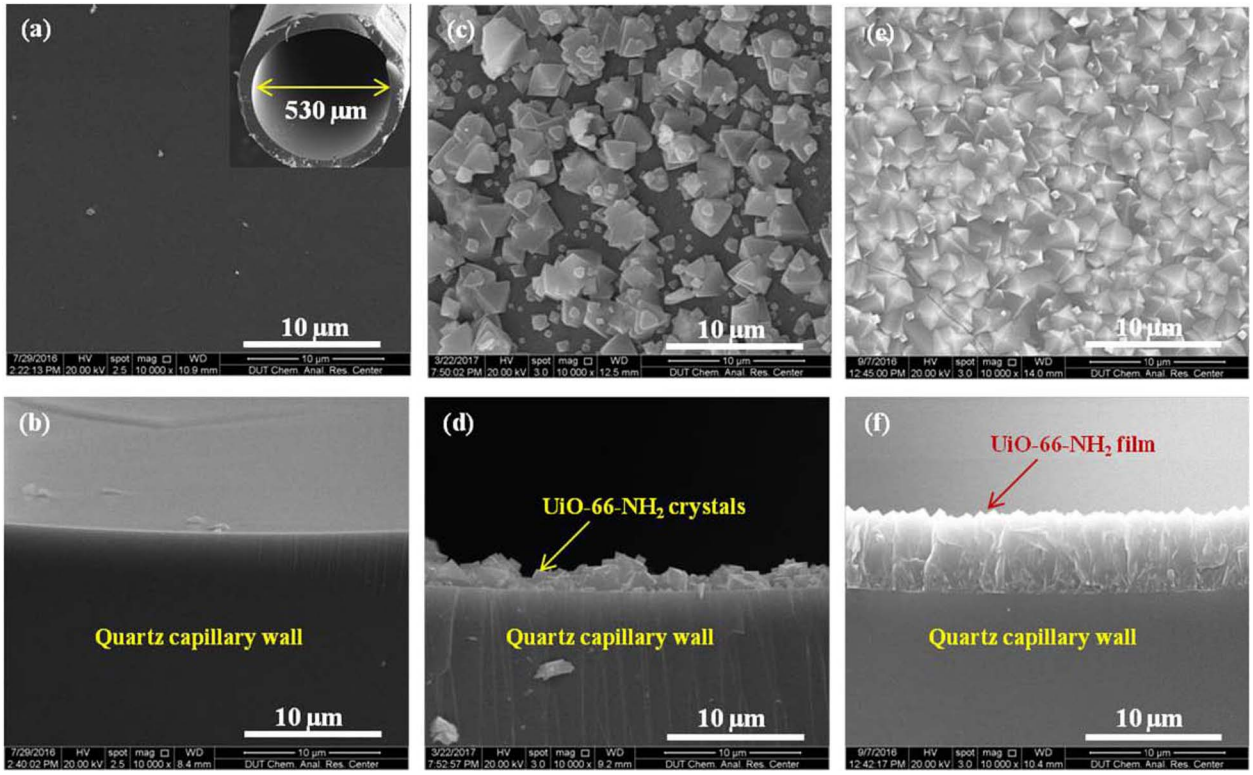

Fig. 3. SEM images of different samples: (a, b) quartz capillary wall (inset: the tube), (c, d) the films grown in-situ on the bare wall and (e, f) the UiO-66-NH_2 films on the wall modified with APTES.

After the modification, a precursor solution with a molar ratio of 1 $ZrCl_4$/1 NH_2-H_2BDC/1 H_2O/500 acetic acid/1000 DMF was prepared and pumped into the capillarytube at a constant flow rate of 0.4 mL/h at 393 K for desired time to obtain a continuous UiO-66-NH_2 film. Finally, the as-synthesized sample was washed by DMF and ethyl alcohol to obtain UiO-66-NH_2 film microreactors. The thicknesses of the films were conveniently controlled by adjusting the synthesis time.

2.2.2. Immobilization of Pd NPs inside the UiO-66-NH_2 film by flow

Pd species were incorporated into UiO-66-NH_2 film to form a Pd/UiO-66-NH_2 film as shown in the setup of Fig. 2. The H_2PdCl_4 aqueous solution (6 mg L^{-1}), prepared by dissolving $PdCl_2$ into HCl aqueous solution, was pumped into the UiO-66-NH_2 film coated capillary microreactor at room temperature (298 K). In order to achieve the Pd/UiO-66-NH_2 films with different Pd contents, the operations were conducted at the flow rate of 1 mL/h for 30 min and 60 min, respectively (remarked as Pd-30/UiO-66-NH_2 and Pd-60/UiO-66-NH_2). Then, DI water was inleted by a flow rate of 3 mL/h to wash the channel for 5 min to remove the unstably immobilized Pd species. Thereafter, fresh $NaBH_4$ aqueous solution (10 mM) was introduced at the flow rate of 2 mL/h for 3 h to reduce the Pd species into Pd NPs. Finally, the prepared microreactor was washed again by DI water at the flow rate of 3 mL/h for 30 min and dried at 373 K for 12 h to achieve Pd/UiO-66-NH_2 film capillary microreactors for the following characterization and reaction.

2.3. Characterization

Scanning electron microscopy (SEM) images of the samples were obtained with a QUANTA 450 (FEI Company) at an acceleration voltage of 30 kV after gold coating. The distribution of elements was identified by energy dispersive X-ray (EDX) using the same QUANTA 450 with an X-MAX 20 mm^2/50 mm^2. The elemental content of Pd was analyzed by inductively coupled plasma-atomic emission spectroscopy (ICP-AES)

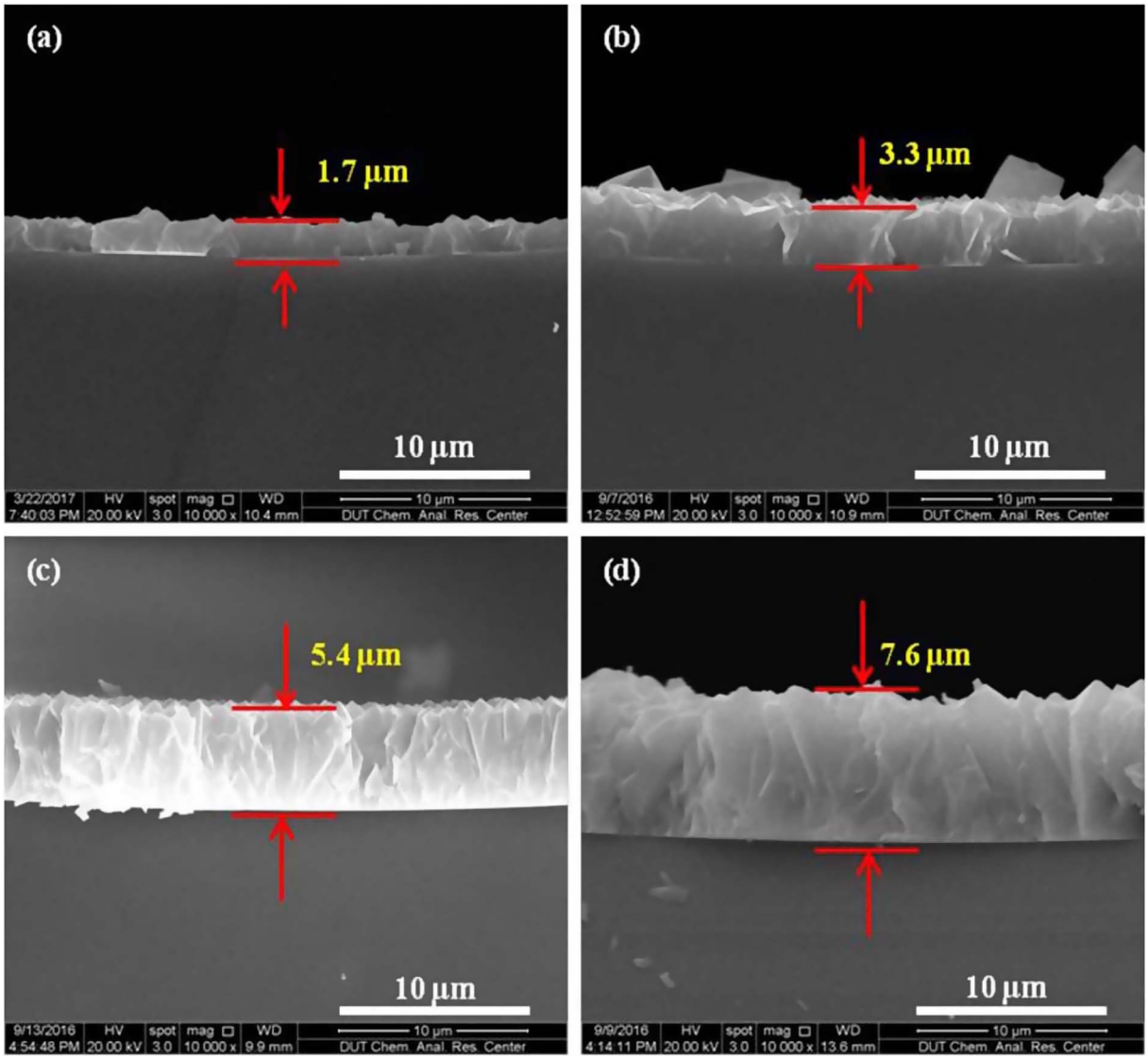

Fig. 4. SEM images of the UiO-66-NH_2 films prepared on quartz capillary wall with APTES modification at 393 K for different synthesis time: (a) 8 h, (b) 12 h, (c) 16 h and (d) 20 h.

using an Optima 2000DV spectrometer. The microstructures of the Pd/UiO-66-NH_2 particles were investigated through transmission electron microscope (TEM) experiments employing a Tecnai F30 (FEI Company). The crystal structures of the samples collected from microreactors were measured by X-ray diffraction (XRD) on a D/max-2400 X-ray diffractometer using Cu-Ka radiation in the range of 5–50° at a scanning rate of 8°/min. The UV spectra were obtained in the range of 250–500 nm by using a UV–vis spectrophotometer (Perkin Elmer, Lambda 750S).

2.4. Catalytic reduction of 4-nitrophenol by continuous flow

As shown in Fig. 2, the resulting Pd/UiO-66-NH_2 film microreactor was installed into the setup. 4-nitrophenol (4-NP) aqueous solution and freshly prepared $NaBH_4$ solution were continuously fed into a tee joint at the same flow rate by two syringe pumps, respectively, and they were mixed into the film microreactor for the reduction reaction at 298 K. The residence time of the reaction was controlled by varying the total flow rate of mixtures in the microreactor. The total flow rate was set as 10, 20, 30, 40, 50 and 60 μL/min, which corresponded to the residence time of 5.31, 2.66, 1.77, 1.33, 1.06 and 0.88 min, respectively. The products, collected from the microreactor outlet, were analyzed by recording absorbance at 399 nm in a quartz cuvette using UV–vis spectrophotometer, and the wavelength range was from 250 nm to 500 nm. The conversion of 4-NP was calculated using the following equation:

$$Conversion\ (\%) = (1-A/A_0) \times 100$$

where A_0 and A are the absorbance of feed and product at 399 nm for 4-NP, respectively.

3. Results and discussion

3.1. Fabrication and characterization of Pd/UiO-66-NH_2 film microreactor

A quartz capillary was selected as the microchannel substrate for the flow growth of Pd/UiO-66-NH_2 film. The inner surface of quartz capillary is quite smooth without any porous structures (Fig. 3a and b). After in-situ growth of UiO-66-NH_2 film as presented in Fig. 3c and d, there are only some accumulations of UiO-66-NH_2 crystals on the inner surface of the quartz capillary. This indicates that it is quite difficult to achieve a continuous and uniform UiO-66-NH_2 film on this kind of substrate by in-situ growth method because of the absence of active nucleation sites for MOFs. To solve above mentioned problem, APTES was introduced as modification regent to activate the inner surface of the quartz capillary before film growth. As expected, a uniform UiO-66-

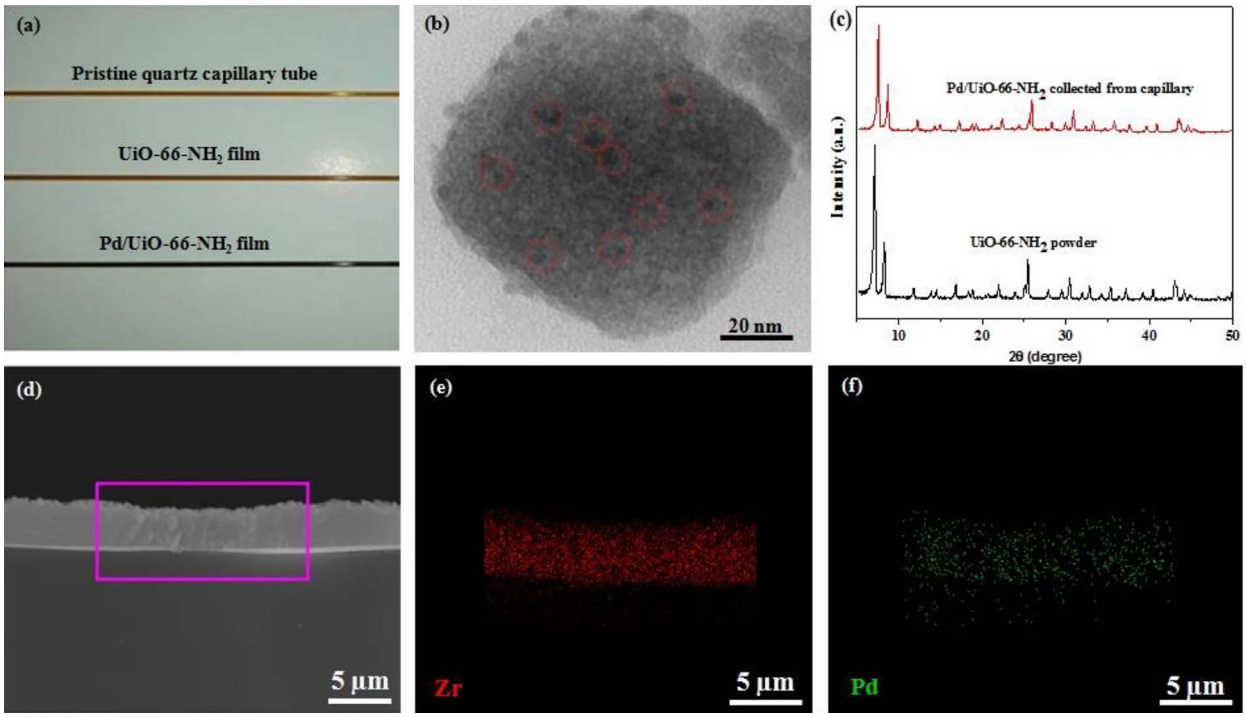

Fig. 5. (a) The images of different quartz capillary tube, (b) the representative TEM microphotograph and (c) XRD patterns of the Pd/UiO-66-NH_2 film, (d) SEM images of Pd/UiO-66-NH_2 film and (e, f) the corresponding element maps.

NH_2 film with the thickness of approximately 6 μm was formed and firmly adhered onto the surface of APTES-modified quartz capillary (Fig. 3e and f). Obviously, APTES plays a key role in formation of the continuous UiO-66-NH_2 film. This can be explained by the fact that the chemically bonded APTES can serve as anchors to capture Zr species, which can greatly enhance the heterogeneous nucleation of UiO-66-NH_2 crystals. By pre-treating with NaOH aqueous solution, the surface of the silica quartz wall is easily activated to produce surface hydroxyl groups, thus providing chemical environment for subsequent modification of APTES. Therefore, APTES can be well grafted on the quartz surface via the combination of hydroxyl group and ethoxyl group. The amino groups of APTES grafted on the wall are favorable for capturing metal cations via metal coordination chelation, which greatly favors the nucleation and growth of MOFs films. This mechanism has been also confirmed in the published literatures [24]. Furthermore, the flow state could provide abundant and fresh synthesis solution uninterruptedly, and thus greatly promote the inter-grown of UiO-66-NH_2 crystals.

It is worth addressing that the thickness of UiO-66-NH_2 film can be conveniently regulated via simply changing the flow synthesis time. As shown in Fig. 4, the films with different thicknesses (1.7, 3.3, 5.4 and 7.6 μm) were achieved after flow synthesis of 8, 12, 16 and 20 h, respectively. Remarkably, the film thickness almost increased linearly with the synthesis time. This advantage is mainly attributed to the fact that flow system can continuously provide high concentration precursors for film growth, and more flow time means longer time for MOFs growth, thus favoring controlling the thickness of UiO-66-NH_2 film via merely adjusting the operation time [25]. It is also suitable for finely adjusting the loading amount of Pd active components by simply changing operation time for the immobilization of Pd NPs.

Based on the possible interaction between the functional amino groups of UiO-66-NH_2 and Pd cations, Pd^{2+} is firstly loaded on UiO-66-NH_2 film and then reduced by $NaBH_4$ aqueous solution under flow conditions to obtain highly efficient Pd/UiO-66-NH_2 film microreactor. The as-prepared UiO-66-NH_2 film with the thickness of about 4 μm was selected to immobilize Pd NPs. As shown in Fig. 5a, after loading Pd NPs on the UiO-66-NH_2 film, the color of the quartz capillary tubes gradually turn from brown to black, while the color of pristine quartz capillary tube is light brown. Transmission electron microscope (TEM) experiments were also carried out to further investigate the microstructure of the Pd/UiO-66-NH_2 particles, which is the subunit of the film. As shown in Fig. 5b, evidently, Pd NPs are dispersed uniformly in the UiO-66-NH_2 and their average size is about 5 nm. XRD patterns (Fig. 5c) of the Pd/UiO-66-NH_2 powder collected from their film counterparts display all of the featured peaks of UiO-66-NH_2, confirming that the crystalline of UiO-66-NH_2 films was well retained during the process of Pd loading. But the characteristic peak of Pd (1 1 1) is not observed at $2\theta = 40.1^\circ$ in the XRD pattern, possibly due to the low Pd content and small diameter of Pd NPs [26]. Furthermore, Elemental analysis of the Pd/UiO-66-NH_2 film was conducted by EDX. From the cross-sectional EDX mapping analysis shown in Fig. 5e and f, which are relevant to the marked area in Fig. 5d, it is obvious that Pd species is highly dispersed in UiO-66-NH_2 film to form an interlaced structure and such structure helps to firmly immobilize Pd NPs and greatly improve the stability of Pd/UiO-66-NH_2 film microreactor. This has also been certified in the following reaction section.

3.2. Catalytic performance

The reduction of 4-nitrophenol (4-NP) to 4-aminophenol (4-AP) was utilized to evaluate the catalytic performance of the achieved Pd/UiO-66-NH_2 film microreactor. For comparison, the UiO-66-NH_2 film microreactor without any Pd catalysts was also investigated for the reduction of 4-NP at the flow rate of 40 μL/min. As shown in Fig. 6a, the absorption peak of 4-NP just slightly drops compared with the original peak of initial 4-NP at 399 nm. No absorption peak of product 4-AP at 299 nm could be seen, indicating that the UiO-66-NH_2 film merely served as catalyst support. As for the slight drop of the absorption peak of 4-NP, the reason can be attributed to the enhanced mass transfer in the microchannel with porous UiO-66-NH_2 film and may be considered as a regular behavior [27]. In general, 4-NP firstly reacts with $NaBH_4$ to produce more reactive 4-nitrophenolate ion (4-NPI), and then 4-NPI converts into 4-AP with the help of Pd catalysts [28]. As expected, for the Pd-60/UiO-66-NH_2 film microreactor containing 0.19 wt% of Pd under the same operation conditions, only absorption peak of 4-AP at

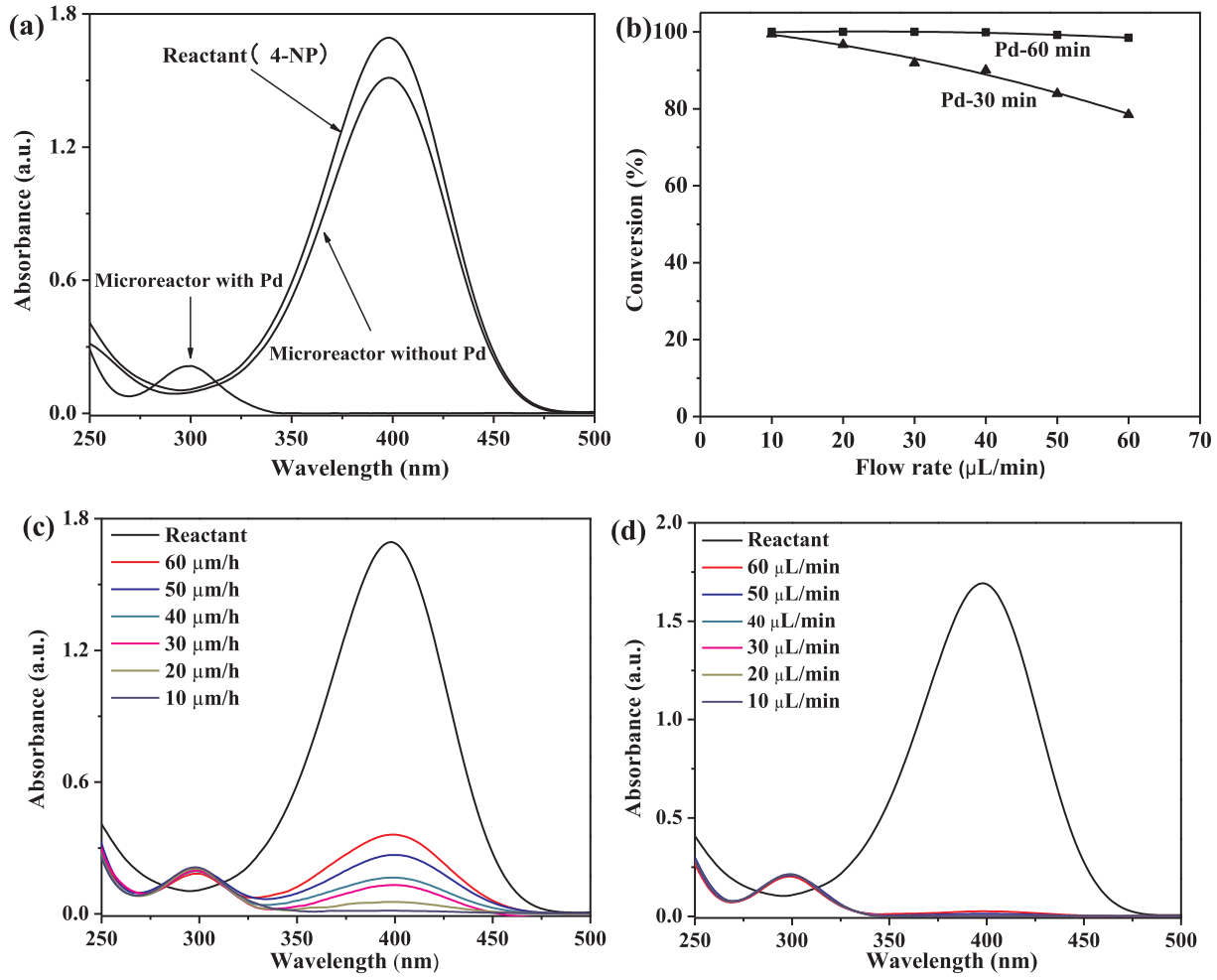

Fig. 6. Catalytic performance of the prepared microreactor with Pd NPs under the inlet 4-nitrophenol concentration of 1 mM at 298 K: (a) comparison of microreactors with and without Pd at the flow rate of 40 μL/min; (b) conversions of 4-nitrophenol in the microreactors with different Pd loadings; (c) UV–vis spectra of Pd-30/UiO-66-NH_2 microreactor under different flow rates; (d) UV–vis spectra of Pd-60/UiO-66-NH_2 microreactor under different flow rates.

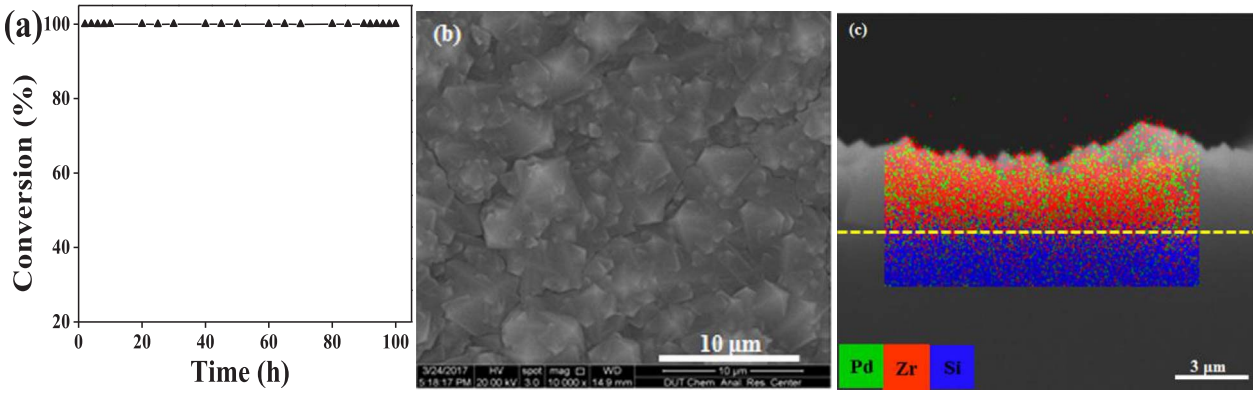

Fig. 7. (a) Catalytic performance of long-term run in the prepared microreactor (Pd-60/UiO-66-NH_2) for 100 h (the flow rate is 30 μL/min and the inlet 4-NP concentration is 1 mM), (b) surface SEM view and (c) cross-sectional EDX mapping analysis of the Pd-60/UiO-66-NH_2 film structure after reaction.

299 nm could be observed. The fractional conversion of 4-NP was calculated to be as high as 100%. This reveals that Pd NPs act as catalytic components on the UiO-66-NH_2 film and show extremely high catalytic activity in this reduction reaction.

In a microreactor, flow rate has a vital influence on the reaction conversion. To illustrate the dependency between conversion and flow rate, two microreactors with different Pd contents (marked as Pd-30/UiO-66-NH_2 and Pd-60/UiO-66-NH_2) have been prepared by changing the flow time for Pd NPs immobilization and then used in the reduction of 4-NP, during which the inlet concentration of 4-NP was fixed at 1 mM. As shown in Fig. 6b, the Pd-30/UiO-66-NH_2 microreactor with 0.10 wt% Pd shows over 99.1% conversion towards 4-NP at the flow rate of 10 μL/min. However, the conversion gradually decreased when increasing the flow rate from 10 to 60 μL/min, and the corresponding UV–vis spectra are shown in Fig. 6c. It is not surprising that the conversion is highest at the lowest flow rate, as the flow rate is opposite to the residence time, which reflects the contact time of the reactants with active components [29–30]. Thus, increasing the flow rate means

decreasing the residence time, leading to the decline of conversion. Compared with Pd-30/UiO-66-NH_2 microreactor, the conversions of 4-NP catalyzed by Pd-60/UiO-66-NH_2 (Pd loading: 0.19 wt%) are nearly 100% at the flow rates ranging from 10 to 40 μL/min, and it slightly declines to 99.4% and 98.5% when the flow rate shifts to 50 and 60 μL/min, respectively (Fig. 6d). It is easy to understand that the Pd-60/UiO-66-NH_2 microreactor can provide enough Pd active components for the reaction, resulting in outstanding catalytic performance at the same condition.

Generally speaking, long-term stability is an essential requirement for the industrial application of capillary reactors. To evaluate the stability of the microreactor, the long-term catalytic performance of Pd-60/UiO-66-NH_2 capillary microreactor was carried out at the flow rate of 30 μL/min and the inlet 4-NP concentration of 1 mM. The long-term operation was conducted for 100 h, during which samples of the outlet were collected every 2 h. Surprisingly, the conversion was always kept at nearly 100% during the entire reaction as shown in Fig. 7a, and this result demonstrates that the capillary microreactor is not only highly efficient but also rather stable for the reduction reaction. SEM image of the surface view from spent Pd-60/UiO-66-NH_2 film shows that this film does not peel off and is not destroyed despite long-time running (Fig. 7b). From cross-sectional EDX mapping analysis (Fig. 7c), the Pd NPs are still uniformly dispersed in the UiO-66-NH_2 film. These results further confirm the excellent stability of the composite structures. The excellent stability is supposed to originate from the fact that the Pd NPs are firmly embedded in the strongly adhered UiO-66-NH_2 film, which should naturally be attributed to our artful strategy for film growth and the high efficiency of UiO-66-NH_2 for the immobilizing Pd NPs.

The above results indicate that the prepared microreactor is a highly efficient, stable and feasible micro-device, which has great potential to be applied for the reduction of 4-nitrophenol (4-NP) to 4-aminophenol (4-AP) in practical applications.

4. Conclusions

In summary, a facile and convenient flow method is developed to fabricate a highly efficient Pd/UiO-66-NH_2 film capillary microreactor for the reduction of 4-NP to 4-AP. This strategy is based on both the flow growth of UiO-66-NH_2 film on the inner wall modified with APTES and anchoring of Pd NPs by functional amino-group of UiO-66-NH_2, leading to a continuous and uniform UiO-66-NH_2 film as well as evenly dispersed and stably fixed Pd NPs in the film. Moreover, both film thickness and loading amount of Pd NPs can be readily adjusted by changing operation time. The resultant Pd/UiO-66-NH_2 film capillary microreactor also retains a conversion of approximate 100% for the reduction of 4-NP during the continuous flow reaction even for 100 h, demonstrating excellent catalytic activity and stability. Our strategy, integrating both MOFs film and Pd NPs into microchannel, has fully exhibited its superiorities in catalysis applications. And it may be extended to the fabrication of other MOFs film-based microchannel loaded with different active components and thus more kinds of efficient microreactors can be achieved.

Acknowledgments

The authors would like to thank the financial support by the Union Funds of National Natural Science Foundation of China and China National Petroleum Corporation (No. U1662101); National Natural Science Foundation of China (No: 21476039).

References

[1] A. Tanimu, S. Jaenicke, K. Alhooshani, Heterogeneous catalysis in continuous flow microreactors: a review of methods and applications, Chem. Eng. J. 327 (2017) 792–821.
[2] S.M. Lai, R.M. Aranda, K.L. Yeung, Knoevenagel condensation reaction in a membrane microreactor, Chem. Commun. 218–219 (2003).
[3] G. Zhang, T. Zhang, X. Zhang, K.L. Yeung, Continuous flow ZIF-8/NaA composite membrane microreactor for efficient Knoevenagel condensation, Catal. Commun. 68 (2015) 93–96.
[4] M. Liu, X. Zhu, R. Chen, Q. Liao, H. Feng, L. Li, Catalytic membrane microreactor with Pd/γ-Al_2O_3 coated PDMS film modified by dopamine for hydrogenation of nitrobenzene, Chem. Eng. J. 301 (2016) 35–41.
[5] T. Zhang, X. Zhang, X. Yan, L. Kong, G. Zhang, H. Liu, J. Qiu, K.L. Yeung, Synthesis of Fe_3O_4@ZIF-8 magnetic core–shell microspheres and their potential application in a capillary microreactor, Chem. Eng. J. 228 (2013) 398–404.
[6] S. Phimsen, H. Yamada, T. Tagawa, W. Kiatkittipong, K. Kiatkittipong, N. Laosiripojana, S. Assabumrungrat, Epoxidation of methyl oleate in a TiO_2 coated-wall capillary microreactor, Chem. Eng. J. 314 (2017) 594–599.
[7] N. Cherkasov, M. Al-Rawashdeh, A.O. Ibhadon, E.V. Rebrov, Scale up study of capillary microreactors in solvent-free semihydrogenation of 2-methyl-3-butynol, Catal. Today 273 (2016) 205–212.
[8] V. Paunovic, V. Ordomsky, M.F.N.D. Angelo, et al., Direct synthesis of hydrogen peroxide over Au–Pd catalyst in a wall-coated microchannel, J. Catal. 309 (2014) 325–332.
[9] Y.Y. Mao, J.W. Li, W. Cao, Y.L. Ying, P. Hu, Y. Liu, L.W. Sun, H.T. Wang, C.H. Jin, X.S. Peng, General incorporation of diverse components inside metal-organic framework thin films at room temperature, Nat. Commun. 5 (2014) 5532.
[10] R.L. Papurello, J.L. Fernández, E.E. Miró, J.M. Zamaro, Microreactor with silver-loaded metal-organic framework films for gas-phase reactions, Chem. Eng. J. 313 (2017) 1468–1476.
[11] H.C. Zhou, J.R. Long, O.M. Yaghi, Introduction to metal-organic frameworks, Chem. Rev. 112 (2012) 673–674.
[12] J. Lee, O.K. Farha, J. Roberts, K.A. Scheidt, S.T. Nguyen, J.T. Hupp, Metal-organic framework materials as catalysts, Chem. Soc. Rev. 38 (2009) 1450–1459.
[13] J.H. Cavka, S. Jakobsen, U. Olsbye, N. Guillou, C. Larberti, Silvia, A new zirconium inorganic building brick forming metal organic frameworks with exceptional stability, J. Am. Chem. Soc. 130 (2008) 13850–13851.
[14] Y. Bai, H.C.Y.B. Dou, L.H. Xie, W. Retledge, J.R. Li, H.C. Cai, Zr-based metal–organic frameworks: design, synthesis, structure, and applications, Chem. Soc. Rev. 45 (2016) 2327–2367.
[15] Z.Y. Guo, C.C. Xiao, R.V.M. Ganese, L. Zhou, T.O. Goh, X.L. Li, D. Tesfagaber, A. Thiel, W.Y. Huang, Pt nanoclusters confined within metal-organic framework cavities for chemoselective cinnamaldehyde hydrogenation, ACS Catal. 4 (2014) 1340–1348.
[16] P.H. Ling, L. Jia, H.X Ju, J.P. Lei, Platinum nanoparticles encapsulated metal–organic frameworks for the electrochemical detection of telomerase activity, Chem. Commun. 52 (2016) 1226–1229.
[17] Y.A. Li, S. Yang, Q.K. Liu, G.J. Chen, J.P. Ma, Y.B. Dong, Pd(0)@UiO-68-AP: chelation-directed bifunctional heterogeneous catalyst for stepwise organic transformations, Chem. Commun. 52 (2016) 6517–6520.
[18] R. Kardanpour, S. Tangestaninejad, V. Mirkhani, M. Moghadam, I.M. Baltork, A.R. Khosropour, F. Zadehahmadi, Highly dispersed palladium nanoparticles supported on amino functionalized metal-organic frameworks as an efficient and reusable catalyst for Suzuki cross-coupling reaction, J. Org. Chem. 761 (2014) 127–133.
[19] S.T. Gao, W.H. Liu, C. Feng, N.Z. Shang, C. Wang, A Ag–Pd alloy supported on an aminefunctionalized UiO-66 as an efficient synergetic catalyst for the dehydrogenation of formic acid at room temperature, Catal. Sci. Technol. 6 (2016) 869–874.
[20] R. Subair, B.P. Tripathi, P. Formanek, F. Simon, P. Uhlmann, M. Stamm, Polydopamine modified membranes with in situ synthesized gold nanoparticles for catalytic and environmental applications, Chem. Eng. J. 295 (2016) 358–369.
[21] L. Zhang, Z. Liu, Y. Wang, R. Xie, X.J. Ju, W. Wang, L.G. Lin, L.Y. Chu, Facile immobilization of Ag nanoparticles on microchannel walls in microreactors for catalytic applications, Chem. Eng. J. 309 (2016) 691–699.
[22] P. Herves, M. Perez-Lorenzo, L.M. Liz-Marzan, et al., ChemInform abstract: catalysis by metallic nanoparticles in aqueous solution: model reactions, Chem. Soc. Rev. 41 (2012) 5577–5587.
[23] R. Javaid, S. Kawasaki, A. Suzuki, T. Suzuki, Simple and rapid hydrogenation of *p*-nitrophenol with aqueous formic acid in catalytic flow reactors, Beilstein J. Org. Chem. 9 (2013) 1156–1163.
[24] A. Huang, N. Wang, J. Caro, Synthesis of multi-layer zeolite LTA membranes with enhanced gas separation performance by using 3-aminopropyltriethox-ysilane as interlayer, Microporous Mesoporous Mater. 164 (2012) 294–301.
[25] X.F. Zhang, Y.G. Liu, Y.S. Liu, K.L. Yeung, W.S. Yang, W.D. Zhu, J.S. Qiu, New membrane architecture with high performance: ZIF-8 membrane supported on vertically aligned ZnO nanorods for gas permeation and separation, Chem. Mater. 26 (2014) 1975–1981.
[26] M.S. El-Shall, V. Abdelsayed, A.E.R.S. Khder, H.M.A. Hassan, H.M. El-Kaderi, T.E. Reich, Metallic and bimetallic nanocatalysts incorporated into highly porous coordination polymer MIL-101, J. Mater. Chem. 19 (2009) 7625–7631.
[27] K.S. Krishna, C.V. Navin, S. Biswas, V. Singh, K. Ham, G.L. Bovenkamp, C.S. Theegala, J.T. Miller, J.J. Spivey, C.S. Kumar, Millifluidics for time-resolved mapping of the growth of gold nanostructures, J. Am. Chem. Soc. 135 (2013) 5450–5456.
[28] E.M. Felix, M. Antoni, I. Pause, S. Schaefer, U. Kunz, N. Weidler, F. Muench, W. Ensinger, Template-based synthesis of metallic Pd nanotubes by electroless deposition and their use as catalysts in the 4-nitrophenol model reaction, Green. Chem. 18 (2016) 558–564.
[29] H. Feng, X. Zhu, R. Chen, Q. Liao, J. Liu, L. Li, High-performance gas-liquid-solid microreactor with polydopamine functionalized surface coated by Pd nanocatalyst for nitrobenzene hydrogenation, Chem. Eng. J. 306 (2016) 1017–1025.
[30] J.F. Ng, Y.T. Nie, G.K. Chuah, S. Janeicke, A wall-coated catalytic capillary microreactor for the direct formation of hydrogen peroxide, J. Catal. 269 (2010) 302–308.